IEEE Robotics and Automation Letters (RAL) paper presented at
2024 IEEE/RSJ International Conference on Intelligent Robots and Systems (IROS)
October 14-18, 2024. Abu Dhabi, UAE

Underwater vibration adhesion by frequency-controlled rigid disc for underwater robotics grasping

Yi Sun, Yangyi Hu, Yi Yang, Min wang, Jiheng Ding, Huayan Pu, Wenchu Jia*

***Abstract*—Underwater adsorption is the key function of underwater robot operation, in order to complete the underwater wall fixation, underwater object capture and other operations. The underwater adhesion mechanism based on vibration control has the advantage of using the liquid viscosity to pull the object surface at a certain distance and control the adhesion effect by frequency. A disc of 0.5mm thickness and 100mm diameter can accommodate the adhesion of different rough planes at 50Hz, a curved cup can be pulled and grabbed at a distance of 7mm at 100Hz, when 0.5mm thick silicone spacers were attached to the bottom of the drive disc, the loading mass of the disc adhesion was increased from 76g to 1056g at a vibration frequency of 150Hz. In short, the underwater vibration adhesion of rigid body is a new adhesion mechanism, which is expected to provide new ideas and applications in the field of underwater grasping.**

***Index Terms*—Underwater wall-climbing robot, Underwater grasping, Underwater vibration adhesion, vibration control.**

I. Introduction

DUE to the huge diversity and potential of ocean resources, the exploration of the ocean is the continuous pursuit of human beings. Therefore, underwater robots play an important role in it [1] [2] [3], underwater adsorption mechanism plays an important role in the collection of resources and wall cleaning [4]. At present, there are three main forms of mature adsorption technology for underwater robots [5] : vacuum adsorption, electromagnetic adsorption and thrust adsorption [6] [7], yet vacuum adsorption requires pre-pressure on the adsorption surface or additional air pump pumping after contact to form a negative pressure. [8] [9] Electromagnetic adsorption cannot adhere to non-magnetic surfaces. Non-contact adsorption based on thrust adsorption requires additional auxiliary fixed elements to prevent high-speed drive components such as propellers from being damaged by impact. [10] [11]

To adapt to wall adsorption or acquisition operations in this environment, a new technology is required. Weston-Dawkes combined Stefan's principle with the principle that the vibration between two planes generates a fluid film [12] through vibration to realize the wall-climbing robot's adsorption scheme in the air. If this adhesion mechanism can be applied to the field of underwater robots, the underwater adhesion mechanism based on the vibration form can not only use the liquid film formed by the fluid to form a negative pressure area to adhere to the object, thus eliminating the dependence on magnetic material. It can also spontaneously realize the adhesion effect within a certain distance through the traction effect, eliminating the limitation that the suction cup needs to apply pre-pressure. Additionally, the vibration form avoids the problem that thrust adsorption is susceptible to damage by high-speed propellers.

To study the cross-fusion of rigid body vibration and the underwater adsorption mechanism. In this paper, we study the possibility of rigid disc adsorption underwater, and find that the adsorption mechanism is traction in the vertical direction, and the adsorption effect is dependent on frequency. The application of the adhesion mechanism is also discussed. The structure of this paper is as follows: the concept of underwater vibration adsorption of rigid disc is proposed. The underwater vibration adsorption experiment is designed from displacement and energy. The application of the traction and adhesion properties for the underwater adhesion mechanism was verified at different frequencies. The relationship between the traction time and the distance is discussed.

II. The concept of underwater vibration adhesion

The theoretical study of underwater vibrations can be traced back to Stefan Adhesion [12]. Inspired by the adhesion principle of barnacles, Stefan. J. proposed Stefan Adhesion, which states that a rigid disc experiences an adhesive force due to the fluid's squeezing viscosity when it separates from a contact surface, and this force is related to the radius of the rigid disc, the gap distance from the wall, and the separation velocity. However, Stefan Adhesion only manifests during the separation process.

Ramanarayanan. S. derived a theoretical explanation based on near-field acoustic levitation, stating that the vibration of a rigid disk in close proximity to a wall in air is influenced by the inherent non linearity introduced by convection and gas comprehensibility, resulting in a time-averaged 'squeeze-film force' [13]. The magnitude of this force is determined by the order of the Naiver-Stokes equation, the comprehensibility coefficient of the fluid, and the local Strouhal number. Weston-Dawkes found that the principle of generating a fluid film in a small gap by vibration can achieve adhesion in the air.

Manuscript received: November 23, 2023; Revised: January 15, 2024; Accepted: April 2, 2024.

This paper was recommended for publication by Editor Júlia Borràs Sol upon evaluation of the Associate Editor and Reviewers'comments.

The authors are with the School of Mechatronic Engineering and Automation, Shanghai University, China. lovvchris@shu.edu.cn

Digital Object Identifier (DOI): see top of this page.

This adhesion mechanism was applied to the wall-climbing robot and a bottle of 3.8 N Coke was hoisted in the air [14]. This theory also applies to water, a typical viscous and incomprehensible fluid. We experimentally verified the feasibility of achieving vibration adhesion underwater.

The process of underwater vibration adhesion is shown in Fig.1. A disc (we called driving disc) is connected to the vibration source and placed in a water-filled tank, and the top surface of the driving disc is a certain depth from the liquid surface. We apply a sine wave signal to the vibration source. The vibration source drives the driving disc to start axial oscillation at a certain frequency. At this time, we place another disc (we called passive disc ,which is as a heavy object) close to the driving disc. We will feel that the passive disc is pulled and spontaneously attached to the driving disc, and adhere to the driving disc. when the driving disc stops vibrating, the passive disc is spontaneously detached by gravity(See Supplementary Movie 1).

We performed a force analysis of the mechanism of traction and adhesion. Vibration drives the flow field movement of the area between the disc and the object. Below the object is regarded as static water. The velocity difference of the flow field on the upper and lower surface of the object forms the pressure difference of the flow field. The upward pressure difference exceeds the resultant force of gravity and buoyancy of the object, and the object is subject to traction, as shown in Fig.1.(b). Then object contact drives the disc to form a fluid membrane. If the carrying capacity of the fluid membrane exceeds the resultant force of gravity and buoyancy of the object, the object can be attached to the vibrating driving disc for a long time. The carrying capacity of the fluid membrane is related to the vibration frequency f of the driving disc, the spacing between the two contact planes h and the radius of the driving disc r, and also has a force in the radial direction (we mainly discuss the force in the vertical direction), as shown in Fig.1.(c).

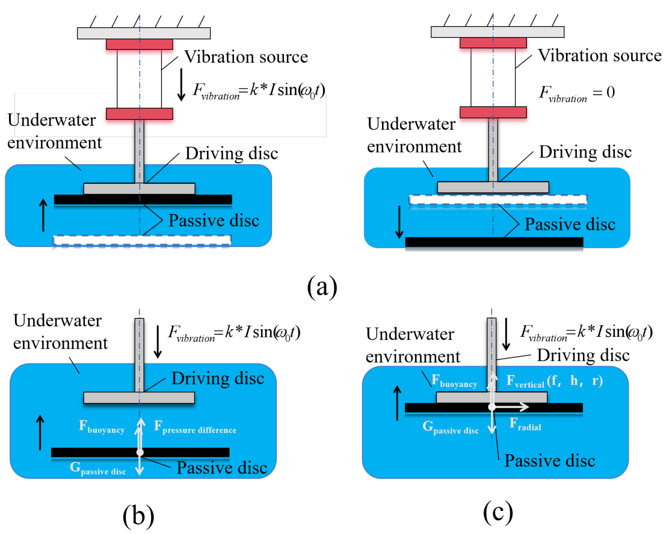

Fig. 1. Adhesion process and force analysis of underwater vibration adhesion Underwater vibration adhesion process. (a) The process of underwater vibration adhesion. (b) Analysis of the forces on objects subjected to traction. (c) Analysis of the forces of the adhesive objects

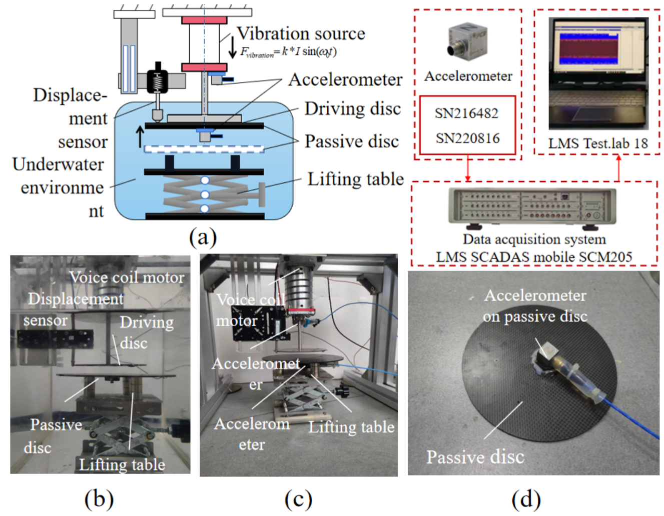

Fig. 2. Design of underwater vibration adhesion experiment:(a) Underwater vibration adhesion platform and experimental design, (b) Arrangement of the displacement sensor, (c) Arrangement of the acceleration sensor, (d) Seal and waterproof treatment of the acceleration sensor

III. Design of Underwater Vibration Adhesion Experiment

The construction of the underwater vibration adhesion experimental platform is shown in Fig.2 (a): We select the voice coil motor HRVM-08-A as the vibration source, and drive the sine wave control signal with controllable output frequency of the voice coil motor through the CME board. The drive current is maintained at 0.7 A. One end of the voice coil motor is connected to the aluminum profile, and the other end is fixedly connected to the drive disc welded with a connecting rod through the flange and the fixed ring. The connected driving disc is placed in the water tank, and a lifting platform is placed in the water tank to undertake the passive disc. The gap between the driving disc and the passive disc is changed by adjusting the height of the lifting platform.

It is difficult to measure the vibration adhesion force under water, so we discuss the role of underwater vibration adhesion mechanism from two angles of displacement and energy , as shown in Fig.2 (b) (c). The motion state of the passive disc can be obtained by the displacement change collected by the contact displacement sensor. Single-frequency Self-Power spectral Density (PSD) and amplitude collected by the acceleration sensor are used to analyze the change of the energy flow direction on the driving disc and the passive disc with time and frequency, as shown in Fig.2 (d).

IV. Result and Discussion

A. Prior Experiment Of Underwater Vibration Adhesion

The size of the passive disc is 2mm in thickness and 75mm in radius. The material is carbon fiber. The net weight of the passive disc plus the acceleration sensor is 84.2g. For the design of the driving disc, we give nine sizes of three thickness and three radius combinations, and use them to explore the frequency range of the adhesion effect. The natural frequency of the vibration source system carrying the driving disc is

TABLE I
ADHESION RESULTS AT DIFFERENT VIBRATION FREQUENCIES

FrequencyHz		50	100	150	200	250	300
thickness(mm)	radius(mm)						
0.5	25	O*	×	×	×	×	×
1	25	O*	×	×	×	×	×
2	25	O*	×	×	×	×	×
0.5	50	O	O*	O	×	×	×
1	50	O	×	×	O	×	×
2	50	O	×	O	×	×	×
0.5	75	O	×	O	×	×	×
1	75	O	×	×	O	×	×
2	75	×	×	×	×	×	×

49.2Hz, and the vibration source vibrates near the natural frequency, which transmits more energy. Therefore, we choose 50 Hz as the gap to explore the influence of the frequency range within 50 to 300 Hz on the vibration adhesion (The drive disc under this condition exhibit less adhesive experimental phenomena at frequencies above 300Hz). The results are shown in Table 1 and Fig.3, where the 'O' can achieve continuous adsorption, '×' indicating that no adhesion effect, '*' indicates that it has traction effect. We also show the four process states of underwater vibration adhesion, namely, initial state, traction adhesion, stable adhesion and stop vibration.

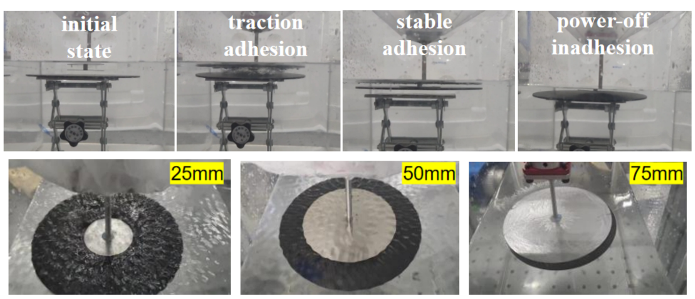

Fig. 3. Four processes of underwater vibration adhesion and Adhesion of three radius driving discs.

B. Analysis Of Underwater Vibration Adhesion Process

The following experiments are designed : A stainless steel drive disc with a thickness of 0.5 mm and a radius of 50 mm (and the drive disc without special instructions in the experiment refers to this disc) is selected as the main research object of underwater vibration adhesion mechanism. The passive disc is 2 mm away from the drive disc before the vibration frequency of 100 Hz is opened. After setting the stopwatch (See Supplementary Movie 2) to ensure the continuity of time, the signal on the camera and the acquisition acceleration sensor is set up and converted into the acceleration amplitude and PSD record and analyze the whole process of underwater vibration adhesion for 15 s by LMS testlab software, and a set of PSD of the driving disc without the passive disc is set as a control. Taking the experiment results in Fig.4a as an example, the underwater vibration adhesion can be divided into four phases. From 0 to 2.66s, the vibration was not activated and the driving and driven discs are all in their initial states; 2.67 to 4.45s is the traction adhesion state ; 4.46

TABLE II
THE FREQUENCY OF THE UNDERWATER VIBRATION ADHESION

Time(s)	Event
0.00-2.66	In the initial preparation stage, the vibration source is not turned on.(the vibration source is power off)
2.67-2.97	Open the vibration source, and the two discs experience changes in acceleration. The first peak appears on the amplitude graph, and bubbles emerge below the driven disc, creating a continuous negative pressure area. At 2.97 seconds, due to uneven force, the passive disc is impacted on the right side, resulting in the first trough and continuously moving closer to the driven disc.
2.98-3.46	As the gap narrows, the number of bubbles decreases and the amplitude of the passive disc increases. The two discs gradually come closer, forming a layer of fluid film (consisting of air and water) to achieve adhesion.
3.47-4.45	After 3.47 seconds, the passive disc comes into full contact with the driven disc, forming a fluid film for complete adhesion. The amplitude shows a second peak, and no visible bubbles are formed thereafter.(the vibration source is power on)
4.46-5.94	After achieving adhesion, the system spontaneously seeks the lowest energy point by moving laterally. The lowest energy point is reached when the right edge of the passive disc aligns vertically with the driven disc.
5.95-11.59	At the lowest energy point, the passive disc undergoes small-scale horizontal reciprocating motion and maintains continuous adhesion.(the vibration source is power on)
11.60-15.00	Disconnect the power supply. After a certain period of adhesion, the passive disc spontaneously detaches at 13.40 seconds and falls onto the lifting platform in the 14.17 s. Subsequently, the compressed bubbles adhering to the passive disc are impacted and ruptured, causing minor impacts on the passive disc.(the vibration source is power off)

to 11.59 s is to achieve a stable adhesion state ; The vibration is stopped after 11.60 s, the passive disk falls falls and creates fluctuations in the 14.17 s bump onto the lifting platformthe results are shown in Fig.4 (a) and Table 2, while Fig.4 (b) represents the change of acceleration amplitude between the driving and passive disks over time, Fig.4 (c) represents the PSD of the driving and passive disks under the same situation, and adds a set of PSD of the driving disc under the passive disc over time.

C. Results And Discussion Of Frequency Effect

The experimental results collected by Table 1 show that different frequencies will result in different adhesion effects. We selected a stainless steel disc with a thickness of 0.5 mm and a radius of 50 mm and 50,100,150 Hz as the experimental object and test frequency. The results collected by the displacement sensor and the acceleration sensor are shown in Fig.5 (a) and Fig.5 (b). Fig.5(a) shows the vertical displacement of the passive disc during the adhesion process at three vibration frequencies. From the perspective of displacement, the adhesion effect is understood as: the smaller the rebound displacement of the passive disc is, the less likely the adhered object is to fall, and the smaller the displacement change of the passive disc vibration is, the more stable the adhesion is.

The displacement change of the passive disc is the smallest at the vibration frequency of 150 Hz, the adsorption is stable, and it is suitable for large loads. The second is 50 Hz, and

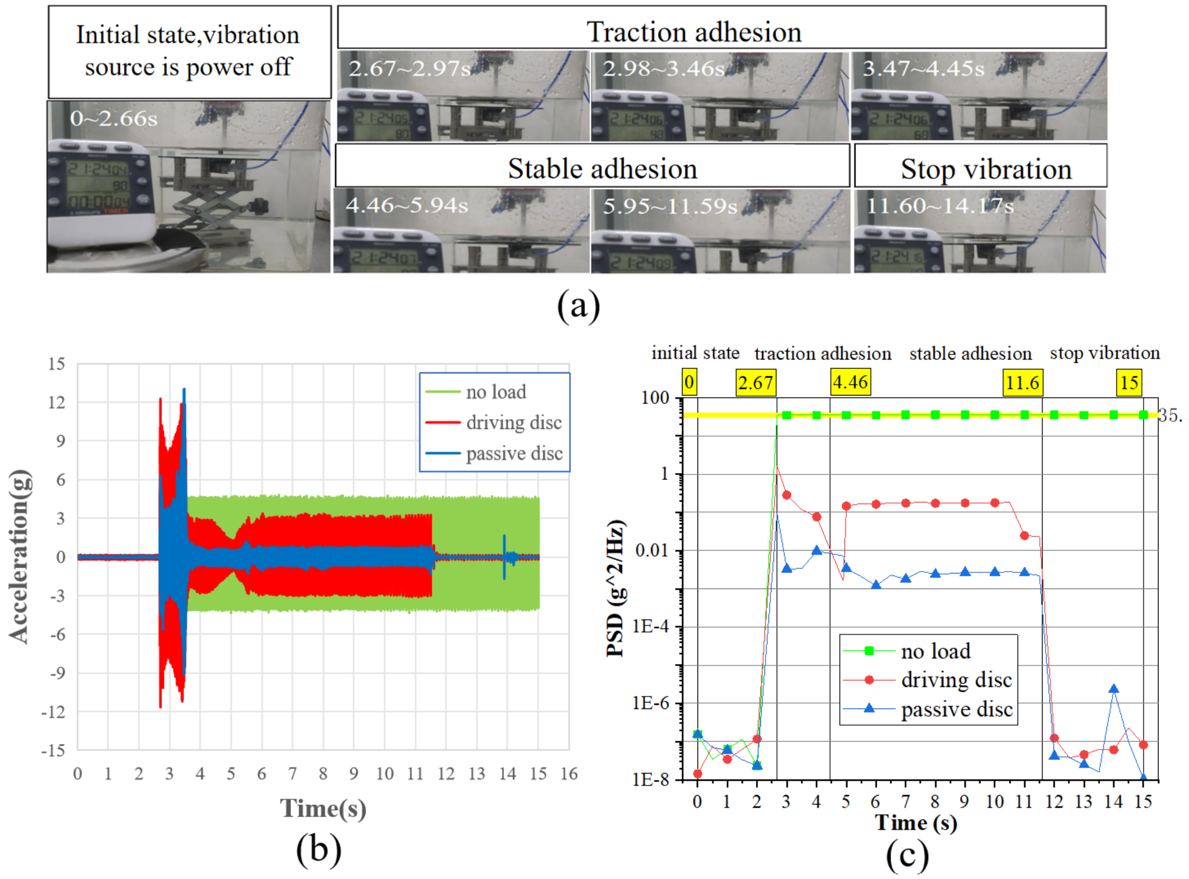

Fig. 4. Analysis of the continuous process of underwater vibration adhesion:(a).Process images of underwater vibration adhesion, (b).Acceleration change on the vibrating disk, (c).PSD changes during the underwater vibrating disc adhesion process

the displacement range of the passive disc is 1.1-1.2 mm. At this frequency, it can be adapted to some cases of concave and convex surface adhesion (this part is verified by experiments in the application test). At the vibration frequency of 100 Hz, the adhesion force of the passive disc is less than the rebound force of the spring probe of the displacement sensor, but the passive disc does not fall. By comparing the PSD of the passive disc in Fig.5 (b), and it shows the PSD distribution of the adhesion between the driving disc and the passive disc in the case of no load. In this case, the PSD distribution on the driving disc is 150 Hz $\geq$ 100 Hz $\geq$ 50 Hz.After achieving stable adhesion, the PSD generated on the driving disc and the passive disc at the 150 Hz vibration frequency is larger than that without load. At this frequency, the passive discs and the driving discs produce a resonance. Combined with the minimum displacement change of the passive disc at the vibration frequency of 150 Hz, we speculate that the resonance of the driving disc with the passive disc helps to maintain the stability of the adhesion.

By comparing the PSD drive performance of the disc in Fig. 5 (b), it is evident that the majority of the energy utilized to generate vibrations by the driving disc is not stored on the passive disc at 50 and 100Hz, but transmitted to the water. Nevertheless, the passive disc remains in its position. We surmise that although the frequencies of 100 Hz are not optimal for the passive disc to adhere, through repeated impact with the water flow, a negative pressure area is created in the lower region of the driving disc. When the passive disc enters this area and the resultant force is less than the tractive force of the negative pressure area, the passive disc is still able to adhere. This results in a tractive effect for the driving disc within a certain distance.

When the vibration frequency is 150Hz, the drive disc has no traction effect, while the drive disc shows traction effect at 50 and 100Hz. Considering that the vibration frequency of the drive disc at 100Hz has the most obvious contrast effect between no-load and adhesion, we choose 100Hz to further explore the effect of the smaller range of frequency change on the adhesion effect, the results are shown in Fig. 5 (c), in the frequency range of 30-180Hz can achieve passive disc adhesion, and by comparing the drive disc no-load case analysis. From the view of the driving disc, except that the resonance frequency of the experimental platform at 50Hz produces a large PSD, in the range of 30-90Hz, the PSD of the driving disc in the underwater no-load decreases with the increase of the frequency, and reaches the minimum value at 80-90Hz, then increases with the increase of the frequency in the range of 100-140Hz, and gradually decreases with the increase of the frequency in the range of 150-170Hz. From the point of view of the passive disc, the change of PSD on the passive disc at 40-140 Hz frequency tends to a horizontal line.

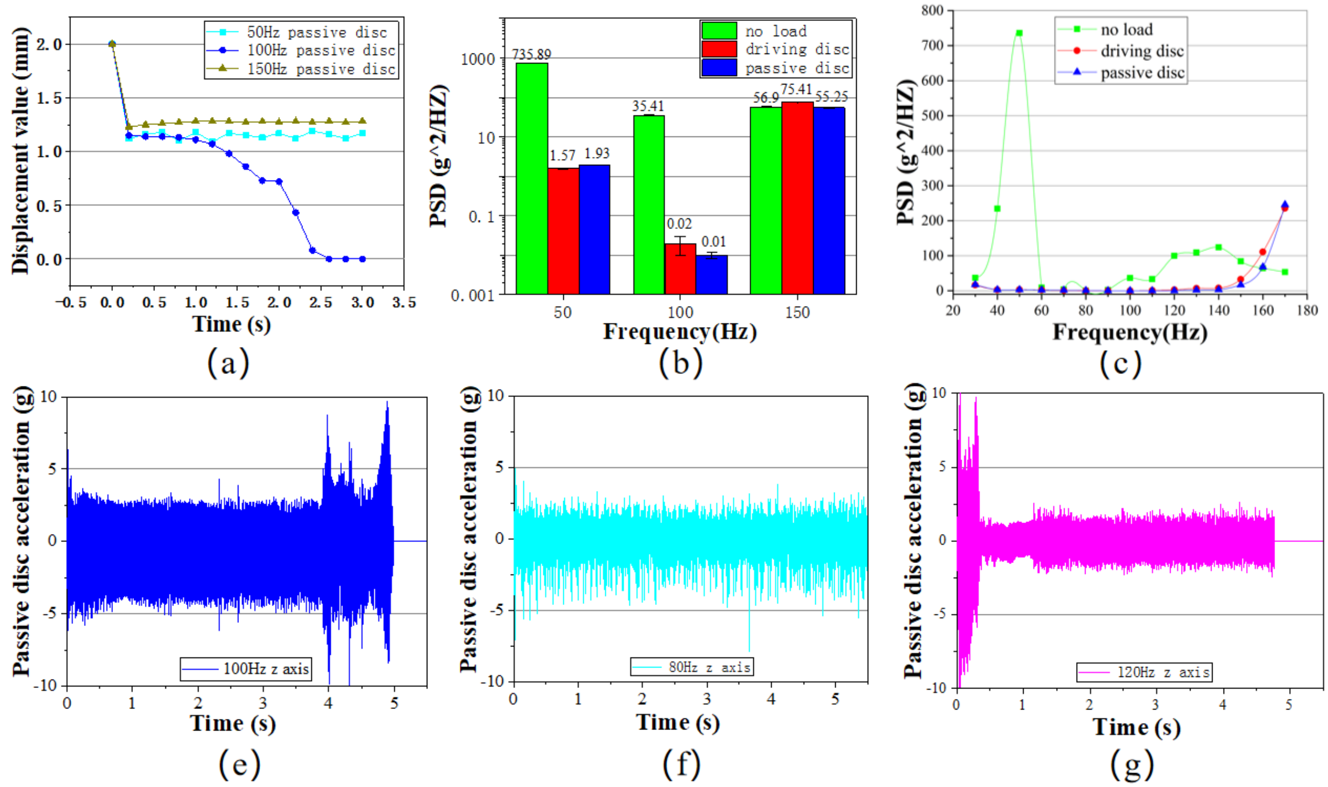

Fig. 5. The curve of displacement and PSD of underwater vibration adhering to passive disk with frequency. (a) Displacement changes of three frequencies. (b) PSD changes at three frequencies.(c) PSD changes in the frequency range of 30 to 180 Hz, (d) Acceleration change in the vertical direction of the passive disk at the 100 Hz vibration frequency, (e) Acceleration change in the vertical direction of the passive disk at the 80Hz vibration frequency, (f) Acceleration change in the vertical direction of the passive disk at the 120Hz vibration frequency.

We selected 80 Hz and 120 Hz two vibration frequencies around 100 Hz to verify and compare with 100 Hz. The results of the acceleration change on the numerical direction (z axis) are shown in Fig.5 (e), (f) and (g). As a control group, the driving disc of 100Hz achieved traction and adhesion to the passive disc within 4 seconds after the open vibration, and the driving disc showed shorter traction and adhesion time than 100 Hz, and the acceleration change curve was consistent with Fig. 4 (b), while at the vibration frequency of 80Hz, the driving disc did not show the traction effect. Meanwhile, we also collected the acceleration change of the passive disc in the horizontal direction (x, y coordinate axis), and found that it was consistent with the numerical direction.After achieving the adhesion effect, the PSD change trends were similar in these three conditions. However, the PSD in different no-load conditions had a significant effect on the traction time. At 80Hz and 120 Hz, the 120 Hz driving disc at 100 Hz and 120 Hz. This was followed by 100 Hz, while the smallest PSD of 80 Hz failed to produce a traction effect. Therefore, we conclude that the initial energy (represented by the PSD) is one of the key indicators affecting the effect of traction and adhesion.

D. Discussion On Traction Distance

The difference between the underwater vibration adhesion mechanism based on frequency control and other adsorption mechanisms lies in the traction effect within a certain distance. [15] [16] [17]Therefore, we explore the traction distance. At the vibration frequency of 100 Hz, the stainless steel with a radius of 50 mm and a thickness of 0.5 mm is used to drive the disc, h represents the distance between the discs, and $h = 0$ is selected as the control group. The measurement starts from $h = 1$ mm and increases in turn at 2 mm intervals. If the driving disc can pull and adhere to the passive disc within 6 seconds and the process of spontaneously finding the lowest point of the ability appears in the acceleration amplitude change of the passive disc (corresponding to the second trough in the traction adhesion process), the corresponding time of the trough is selected as the time point to achieve stable adhesion. If the passive disc does not adhere beyond this time, it is considered as no traction. It is found that the critical value is 5 to 7mm, and the perception of the grasping object or the adhesion wall on the driving disc is of practical value for the underwater vibration adhesion applied to the underwater robot. However, it is not enough to judge the motion only from the perspective of the change of acceleration amplitude. Therefore, we use PSD as the criterion to verify the synchronous state of the driving disc and the passive disc through the energy point of view, and find the feasibility of traction adhesion from the energy point of view. We collected the change of PSD on the driving and passive discs with time, and recorded the change process of traction to adhesion at five distances, as shown in Fig.6 :

Fig.6 (a) shows the acceleration change on the passive disc under five kinds of clearances from 0 to 7mm ; Fig.6 (b) shows the change of PSD on the passive disc in the same situation, $h = 0$, the acceleration change of the passive disc is stable ; when $5 \geq h \geq 1$ mm, the acceleration change of the passive disc during the traction period is greater than the change of the stable adhesion, and the greater the h, the longer the time from traction to adhesion ; when $h = 7$ mm,At this time, the passive disk is not pulled, and the change of response amplitude is the effect of the vibration drive disk hitting the water flow. In Fig.6 (b), the PSD change curve of the passive disc with five spacings can be seen. The PSD of the passive disc that can produce adhesion is mainly stabilized at 0.17 g^2/ Hz after adhesion, while the PSD of the distance that cannot be adhered is affected by the acceleration change of water flow. For the case of distance $h = 1$ mm, the PSD with adhesion lower than other spacings may be affected by the surface of the lifting platform on the bottom surface of the passive disc.

Fig.6 (c) shows the change of PSD on the driving disc under the same conditions. From the 7mm gap, we can see that the PSD on the driving disc that produces adhesion is two orders of magnitude smaller than the PSD that does not achieve adhesion, that is, the energy on the driving disc that does not achieve adhesion is not converted to adhesion. The PSD of no-load tap water can reach $80g^2$/ Hz at a distance of 7mm from the lifting platform, and compared with fig.8 (d), it can be seen that in the three cases of always maintaining adhesion ($h = 0$), traction and adhesion ($h = 5$ mm) and non-adhesion ($h = 7$ mm). The PSD changes of the driving disc and the passive disc are synchronous.

V. Discussion

In light of the unique characteristics of the underwater vibration adhesion mechanism in generating traction and adhesion, as illustrated in Fig.7, we conducted practical experiments to explore the optimal vibration frequency for achieving these effects. To investigate the mechanism of object manipulation, we subjected straw cups to pulling tests at 100Hz with a vertical distance of 7mm. Given the challenge of observing traction effects at 50Hz visually, we increased the separation between the driving disc and passive disc to 25mm and dispersed small particles with water-like density on the passive disc. By tracking the trajectory of these particles, we could visually demonstrate the impact of flow field variations. Following 9 seconds of 50Hz vibration, we observed the appearance of yellow rice grains on the upper surface of the driving disc, offering a novel boundary condition assumption for our subsequent fluid simulation studies. Moreover, at the 50Hz vibration frequency, the driving disc exhibited adhesion forces towards shells, rough surfaces, and other objects. Lastly, by integrating the underwater vibration adhesion mechanism with a delta robot, we successfully achieved the underwater grasping of a stainless steel disc (Refer to Supplementary Movie 3).

Following the test results, it was discovered that incorporating soft materials onto rigid discs can significantly expand the frequency range and improve the effectiveness of adhesion. We conducted experiments to assess the load capacity of rigid adhesion across three different vibration frequencies by incrementally increasing the weight on the passive disc. The adhesion performance under these conditions served as the control group. Subsequently, under identical conditions, we repeated the load capacity tests with a 50mm radius and 0.5mm thickness silicone pad added to the bottom of the driving disc. The outcomes of these tests are presented in Fig.8.

The introduction of silicone pads led to a notable enhancement in the load capacity of the driving disc across all three vibration frequencies. Particularly at 150Hz, the adhesion force exerted by the driving disc saw a ten-fold increase, rendering the passive disc unable to detach within two seconds of power disconnection. We hypothesize that the inclusion of soft materials may have induced alterations in the fluidic membrane, or potentially introduced additional microscopic-level adhesion mechanisms that bolster the adhesion force generated by the driving disc.

Underwater vibration adhesion is a new underwater attachment mechanism, although it is like a combination of the thrust adsorption mechanism [11] [8] and the passive vibrating suction cup [5] mechanism. In principle, underwater vibration adhesion mechanism and thrust adsorption is by controlling the movement of fluid in different areas of the pressure difference of negative pressure effect of attachment, they are not contact adsorption mechanism, but from the form of motion, thrust adsorption control fluid way from the rotation of the propeller, underwater vibration adhesion control fluid is driven disc straight vibration. By means of linear vibration, negative pressure characteristics of underwater vibration adhesion and the working way of passive vibration suction cup is similar, but the principle of passive vibration suction cup attachment mainly comes from the negative pressure mechanism of the suction cup, and the principle of underwater vibration adhesion attachment from the bearing capacity of the fluid film and the motion flow field pressure difference.

In the application of underwater robot, thrust adsorption is more suitable for the adsorption of wall climbing robot, while underwater vibration adhesion is more suitable for the capture of underwater objects. Prof.Guo proposed innovative sliding negative pressure adsorptive approach applied to an underwater climbing adsorption robot [8]the results show that the robot can generate a maximum adsorption force of 600kg at a gap height of 12mm in adsorption mode, and can maintain a maximum force of 363kg at a gap height of 28mm in locomotion mode. However, this adsorption mechanism cannot apply and underwater actuator grab, otherwise some smaller objects will be involved in the propeller caused damage to the underwater adsorption robot, despite the currently demonstrated traction distance of underwater vibration adhesion is only in 5 to 7mm gap traction because of the motor power limitations. We don't have to worry about the generation of negative pressure of vibration will damage the vibration source.

We tried to compare the adsorption effect of underwater vibration adhesion with that of passive vibrating suction cups [5]. Although the underwater vibration absorption module has a maximum adsorption force of 18N, the weight of the whole

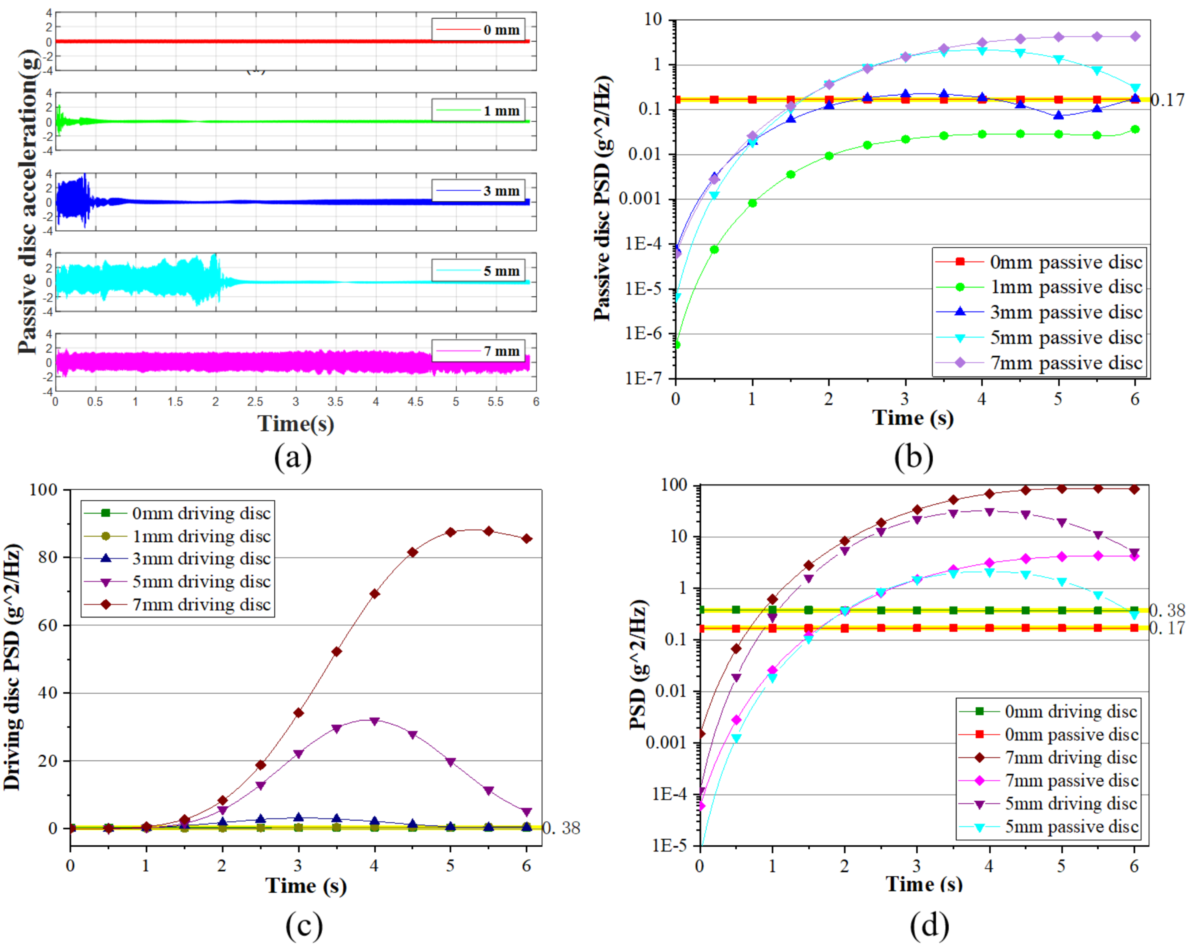

Fig. 6. The variation of underwater vibration traction time with spacing and the synchronization of driving and passive discs.(a). Acceleration change of five kinds of spacing; (b)The change of PSD of five kinds of gap passive discs; (c)The change of PSD of the driving disc with five kinds of clearances; (d)The synchronous curve of PSD of driving and passive discs with the change of gap.

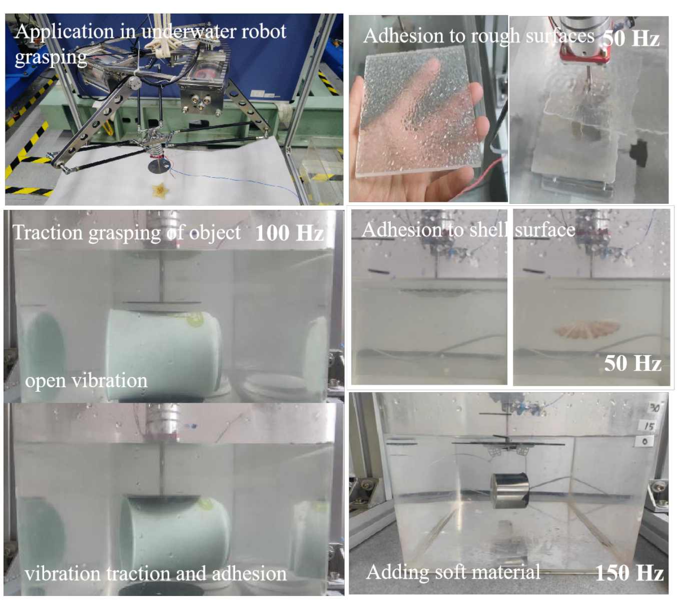

Fig. 7. Application of different frequencies of the underwater adhesion mechanism.

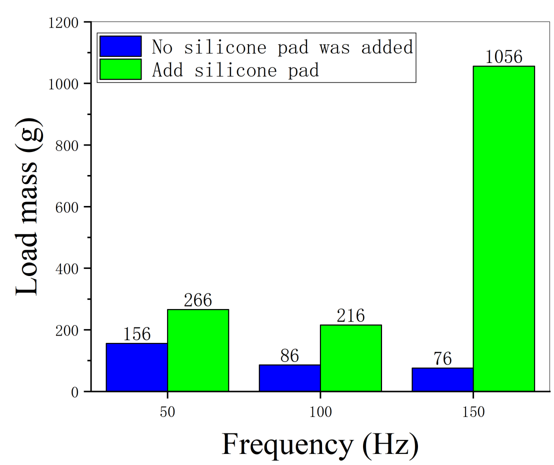

Fig. 8. Effect of adding the soft material on the adhesion force.

machine reaches 676g without the control original for the mass, adsorption force of the unit mass is 26.63N/kg. Underwater vibration adhesion module can produce an adsorption force up to 10.34N, but the mass of whole machine is 128g without the control original, The adsorption force per unit mass that is up to 80.78N/kg, Thus, in the case of generating the same adhesion force magnitude, The method of underwater vibration adhesion is more energy-saving.

The adhesion mechanism of contrast underwater vibration produces an adhesion force of 10N, the method of octopus-inspired adhesive skins for intelligent and rapidly switchable underwater adhesion [18] need only the size of five fingers area, the mechanism needs to apply at least 3N pretension force, and adsorption rapid switching need to use gas pump. limited by the air tightness in underwater, we think underwater vibration adhesion mechanism only need to open and close the vibration switch, which can achieve adhesion and inadhesion state. And we can achieve traction on objects within a certain distance, in this case we do not need additional pretension force.

Of course, we also have some concerns about the underwater vibration adhesion mechanism, the vibration source of underwater vibration adhesion mechanism compared with smaller or even microscopic adsorption area is an advantage we do not have, such as the Elasticity-enhanced wet attachment of biomimetic microcup structures [19], Yue Wang Designed a suction cup with a radius of 120 microns. This suction uses the force between water molecules to produce a negative pressure of 0.3 Mpa. However, compared with the active suction cup, we are more concise, and do not have to consider the tightness and carrying of the gas pump.

There is also a major concern, the adhesion force of the underwater vibration adhesion mechanism is not only related to the vibration, also influenced by the interface materials and fluid media. Our test found that the underwater vibration mechanism does not achieve adhesion in the air, and for some fluids with high viscosity (such as silicone oil, etc.), we need to consume more energy to make the fluid move to achieve continuous adhesion. At the same time, it is difficult to grasp some irregular shaped objects only with the existing vertical adhesion force.

VI. Conclusion

We found an underwater vibration adhesion mechanism through experiments, and explored the two steps of adhesion and traction respectively from the perspective of frequency. Some interesting applications are obtained: a 0.5mm thick disc with a diameter of 100mm has the capacity to adhere to rough surfaces at 50Hz. At 100Hz, a concave cup can be pulled and held at a distance of 7mm. When 0.5mm thick silicone spacers were affixed to the underside of the disc, the adhesion force of the disc increased from 76g to 1056g at a vibration frequency of 150Hz. In our future studies, we plan to compare the lateral arrangement of the vibration source or explore alternative configurations to further enhance the adhesive capacity. Additionally, we envision applying this adhesion mechanism to underwater grasping.

Acknowledgments

This work was partially supported by the National Key Research and Development Program of China (Grant No. 2020YFB1313000); the National Natural Science Foundation of China (Grant Nos. 61873157, 61922053, U2013202, 61903242); and the Program of Young Eastern Scholar of Shanghai, China (Grant No. GD2016031).

References

[1] Sanjib Kumar Deb, Jahed Hossen Rokky, Tuton Chandra Mallick, and Juliana Shetara. Design and construction of an underwater robot. pages 281–284, 2017.

[2] Zizhou Lao, Yuanfeng Han, Yunshan Ma, and Gregory S. Chirikjian. A learning-based approach for estimating inertial properties of unknown objects from encoder discrepancies. *IEEE Robotics and Automation Letters*, 8(9):5283–5290, 2023.

[3] Yangzhou Jiang, Chong Li, Yujian Tong, and Jiwen Fang. Design and simulation analysis of piezoelectric driven underwater robots. In *2022 16th Symposium on Piezoelectricity, Acoustic Waves, and Device Applications (SPAWDA)*, pages 157–163, 2022.

[4] Afshin Falsafi. The science and mechanics of adhesion: An industrial view. *Dental Materials*, 39, 06 2023.

[5] Rui Chen, Qianqian Fu, Ziyi Liu, Xiuqi Hu, Min Liu, and Ruizhou Song. Design and experimental research of an underwater vibration suction module inspired by octopus suckers. *2017 IEEE International Conference on Robotics and Biomimetics*, 12 2017.

[6] Hao Yan, Qizhi Yin, Junfa Peng, and Bo Bai. “multi-functional tugboat for monitoring and cleaning bottom fouling”. *IOP Conference Series: Earth and Environmental Science*, 237:022045, 03 2019.

[7] Yaohui Xu, Kai He, WenLiang Zhao, Haitao Fang, Qiyang Zuo, and Zheng Li. “a novel design of a wall-climbing robot and experimental study on magnetic wheels”. *2021 International Conference on Computer, Control and Robotics (ICCCR)*, pages 60–65, 01 2021.

[8] Tingting Guo, Xiuyan Liu, and Song Dalei. “innovative sliding negative pressure adsorptive approach applied to an underwater climbing adsorption robot”. *Physics of Fluids*, 33:117107, 11 2021.

[9] Jessica Sandoval, Michael Ishida, Saurabh Jadhav, Sidney Huen, and Michael Tolley. Tuning the morphology of suction discs to enable directional adhesion for locomotion in wet environments. *Soft Robotics*, 9, 03 2022.

[10] Yawei Zhu, RenGuan Zhou, Yang Gang, YanQing Zhu, and Dean Hu. “experimental and numerical study of the adsorption performance of a vortex suction device using water-swirling flow”. *Science China Technological Sciences*, 63, 04 2020.

[11] Yanhu Chen, Siyue Liu, Luning Zhang, Peiyang Zheng, and Canjun Yang. Study on the adsorption performance of underwater propeller-driven bernoulli adsorption device. *Ocean Engineering*, 266:112724, 12 2022.

[12] J. Stefan. Versuche über die scheinbare adhäsion. *Annalen der Physik*, 230(2):316–318, 1875.

[13] S. Ramanarayanan, Wilfried Coenen, and A.L. Sánchez. “viscoacoustic squeeze-film force on a rigid disk undergoing small axial oscillations”. *Journal of Fluid Mechanics*, 933, 02 2022.

[14] William Weston-Dawkes, Iman Adibnazari, Yi-Wen Hu, Michael Everman, Nick Gravish, and Michael Tolley. “gas-lubricated vibration-based adhesion for robotics”. *Advanced Intelligent Systems*, 3, 05 2021.

[15] Weiwang Duan, Zhilin Yu, Wenhui Cui, Zengxin Zhang, Wenling Zhang, and Yu Tian. Bio-inspired switchable soft adhesion for the boost of adhesive surfaces and robotics applications: A brief review. *Advances in Colloid and Interface Science*, 313:102862, 02 2023.

[16] Julian Langowski, Dimitra Dodou, Marleen Kamperman, and Johan L Van Leeuwen. Tree frog attachment: Mechanisms, challenges, and perspectives. *Frontiers in Zoology*, 15, 08 2018.

[17] Elliot Hawkes, Eric Eason, David Christensen, and Mark Cutkosky. Human climbing with efficiently scaled gecko-inspired dry adhesives. *Journal of the Royal Society, Interface / the Royal Society*, 12, 01 2015.

[18] Sean Frey, A B M Tahidul Haque, Ravi Tutika, Eric Markvicka, and Michael” Bartlett. “octopus-inspired adhesive skins for intelligent and rapidly switchable underwater adhesion”. *Science Advances*, 8:eabq1905, 07 2022.

[19] Yue Wang, Zhengwei Li, Mohamed Elhebeary, René Hensel, Eduard Arzt, and M Saif. “water as a ”glue”: Elasticity-enhanced wet attachment of biomimetic microcup structures”. *Science advances*, 8:eabm9341, 03 2022.